

Architectural characteristics of the normal and deformity mandible revealed by three-dimensional functional unit analysis

Wonse Park · Bong-Chul Kim · Hyung-Seog Yu ·
Choong-Kook Yi · Sang-Hwy Lee

Received: 19 January 2009 / Accepted: 21 September 2009 / Published online: 13 October 2009
© Springer-Verlag 2009

Abstract The 3D architecture of the mandible contributes to the functional and morphological characteristics of the lower one third of craniofacial region. The mandible has six distinct functional units, and its architecture is the sum of balanced growth of each functional unit and surrounding matrix. A dentofacial deformity (DFD) with malocclusion can be interpreted as their unbalanced growth. In order to characterize the mandibular 3D architecture, we analyzed the 3D reconstructed computed tomography (CT) images in terms of functional units. We evaluated both sides of 30 datasets of 3D CT scans of normal controls ($N=6$) and patients with prognathic ($N=17$) or retrognathic ($N=7$) mandibles. We first identified and evaluated reference points to define mandibular functional units and compared

their linear and angular measurements of DFD with normal group. The condylar and body length, the ratio of condyle/coronoid length, and the condylar head axis angle showed the statistically significant differences between groups. From these results, we could define the 3D reference points for functional units and identify the 3D architectural characteristics of DFD mandibles. These models may help us improve diagnosis and treatment planning to let them return to the normal and balanced architecture for DFD.

Keywords Mandible · Three-dimensional · Functional unit · Computed tomography · Dentofacial deformity · Reference point

W. Park

Department of Advanced General Dentistry,
and Human Identification Research Center,
College of Dentistry, Yonsei University,
Seoul, South Korea

B.-C. Kim · C.-K. Yi

Department of Oral and Maxillofacial Surgery,
College of Dentistry, Yonsei University,
Seoul, South Korea

H.-S. Yu

Department of Orthodontics, College of Dentistry,
Yonsei University,
Seoul, South Korea

S.-H. Lee (✉)

Department of Oral and Maxillofacial Surgery,
Oral Science Research Center and Oral Cancer Research Center,
College of Dentistry, Yonsei University,
134 Shinchondong, Seodaemun-Gu,
120-752 Seoul, South Korea
e-mail: sanghwy@yuhs.ac

Introduction

The mandible is the U-shaped lower jaw bone with biarthroidal temporomandibular joints. It occupies most of the lower face, and its architectural characteristics [1] significantly influence facial appearance and the jaw function. Its abnormal or unbalanced growth causes dentofacial deformity (DFD) and malocclusion [2].

Architecture in biology denotes a basic structural form and specifically refers to the morphology and orientation of skeletal structures [3, 4]. The mandible is first shaped during the embryonic development of the first pharyngeal arch, with the formation of Meckel's cartilage of mesodermal origin and the intramembranous bone of mesenchymal origin [5]. The embryonic mandible continues to develop as the secondary cartilage is laid down at the condyle, coronoid, and symphyseal area, each of which will later form a functional unit. After birth, the mandibular architecture is modified by growth, mainly composed of

condylar displacement and superficial apposition and resorption [6, 7].

Functional units were first described by Moss, with the mandible having six functional growth units: the symphysis, body, dentoalveolus, angle, coronoid, and condyle [8, 9]. Each unit is affected by the surrounding functional matrix, and the overall mandibular growth is a sum of the independent growth of each unit [1]. In addition, the balance of the condylar and coronoid unit contributes most to normal or abnormal growth, as indicated by studies of 2D radiography [10].

Traditional 2D radiographies have been main tool for DFD [1, 3, 11] while the developing 3D technology is rapidly catching it up [12–16]. The 2D radiography has inevitable limitations in describing the DFD due to its 2D expression of 3D object to bring about the possible inaccuracy, invisibility, distortion, or other limitations. So if we evaluate the units of mandibular architecture in DFD using 3D technology, we may better understand the characteristics and patterns of this deformity. Such an understanding may also benefit the comprehensive 3D treatment aimed at restoring normal and balanced architecture.

Thus, we conducted a 3D analysis of normal and deformed mandibles, by functional units. We first identified reference points that defined each architectural and functional unit. Then, we measured and compared the lengths and angles of the mandibular units on the 3D images made from computed tomography (CT) scans. From these works, we could identify the 3D architectural characteristics of the DFD mandible for the improved diagnosis and treatment planning of the DFD.

Materials and methods

Patients

This work was approved by the local ethics committee of Dental Hospital, Yonsei University, Seoul, Korea (IRB number 2-2006-0004).

Group I (normal control)

Six young, healthy volunteers (mean age 19.5 years, three males and three females) were enrolled in the study. Clinical and cephalometric examinations with a dental cast were used to rule out DFD and malocclusion. On clinical examination, those who showed any facial disharmony, facial asymmetry, or history of orthodontic treatment were excluded. We also performed the architectural and structural analysis of Delaire et al. [3] on the lateral cephalograms to validate the normal position of the maxilla and mandible.

Group II (mandibular retrognathism) and group III (mandibular prognathism)

Patients ($N=24$, 13 male and 11 female) were selected who visited the Department of Oral and Maxillofacial Surgery of Yonsei University Dental Hospital for the treatment of DFD and malocclusion. They were evaluated by the same protocols used for normal volunteers, as described above, and assigned to group II ($N=7$, mean age 23.8 years old) or group III ($N=17$, mean age 21.7 years old).

Image acquisition and 3D reconstruction

All participants in all groups underwent CT imaging. On the CT machine, participants were positioned with the Frankfort horizontal (FH) line perpendicular to the floor and the facial midline parallel to the long axis of the CT machine. The imaging was performed with a CT Hi-speed Advantage (GE Medical System, Milwaukee, WI, USA) with a high-resolution bone algorithm, 512×512 matrices, 120 KVP, and 200 mA. The images were scanned from the top of the cranial vault to the chin. The thickness of the axial images was 3 mm, the table speed was 6 mm/s, and the 3D image was reconstructed with 2-mm slices.

The acquired digital image and communications in medicine data were sent to a personal computer with Intel Pentium 4 with 1.6 GHz CPU, 1 GB RAM, 250 GB hard drive, and Microsoft Windows XP OS. Reformatted 3D images were created using Coreplan 3D[®] software (Seoul C&J Inc., Seoul, South Korea).

Reference points and planes for the 3D functional unit analysis

To establish the midsagittal reference plane on the reconstructed 3D CT images, we used three reference points: the foramen cecum, sella, and basion. For the horizontal reference plane, we used the Frankfort plane, defined by bilateral orbitalia and the right porion.

For the architectural analysis on 3D CT, we evaluated different possible reference points that could be used to define growth units. These points are summarized and depicted in Table 1 and Fig. 1. We began by choosing three potential points to represent the mandibular foramen because this structure is useful in evaluating the growth patterns of three functional units: the condyle, coronoid, and body. The potential points were the tip point of the lingula (T), the fossa of the foramen (F), and an imaginary central point of the foramen entrance (C). We measured the distances from each of these points to the most superior point of condyle (CON) and the tip of the coronoid process (COR) and defined each distance as CON-T, COR-T,

Table 1 Reference points used in this study

Landmark		Definition
FC	Foramen cecum	The most superior point of the foramen cecum lies between the crista galli and the crest of the frontal bone
S	Sella	The center of the hypophyseal fossa
Ba	Basion	The most anterior point of the foramen magnum
Or	Orbitale	The lowest point of each infraorbital margin
Po	Porion	The most superior point of the right external auditory meatus
T	Apex of lingula	The apical tip of the lingula around the mandibular foramen
F	Fossa of mandibular foramen	The most inferior point of the mandibular foramen fossa
C	Center point of mandibular foramen	The imaginary center of entrance of the mandibular foramen
CON	Condyle	The most superior point of the mandibular condyle
CON_l	Lateral pole of condyle	The most lateral point of the mandibular condyle
CON_m	Medial pole of condyle	The most medial point of the mandibular condyle
Go	Gonion	The most prominent, inferior, and posterior point at the angle of the mandible
MF	Mental foramen	The entrance of the mental foramen
MAS_ant	Masseter-anterior	The most anterior point of the masseter muscle at the mandibular angle
Pog	Pogonion	The most anterior midpoint of the symphysis of mandible

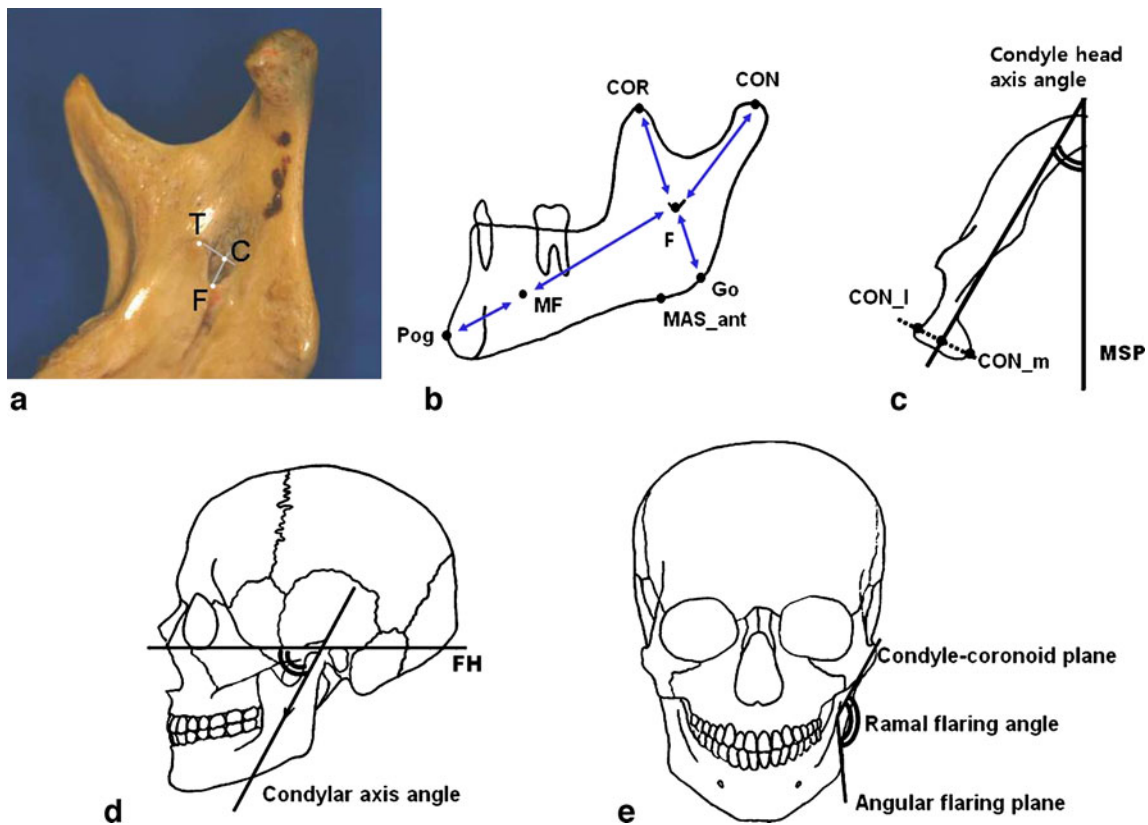


Fig. 1 The reference points for the functional units and the measurements in lengths, planes, and angles of the units. **a** Three candidate reference points for the mandibular foramen. **b** The reference points seen from the lateral aspect, with linear measurements. **c** The reference

points seen from the inferior aspect, showing the condyle head axis angle. **d** Condylar axis angle. **e** Condyle–coronoid plane, angular flaring plane, and ramal flaring angle

CON-F, COR-F, CON-C, and COR-C (Table 2). All measurements were repeated five times per week for 3 weeks on the same CT images by one author; the discrepancies between the measurements were used to evaluate reliability of each term based on the reproducibility of the points and distances mentioned above.

We also included different reference points to represent the condyle, including the most superior (CON), lateral (CON-l), or medial point (CON-m) of the condylar head. The reference point for coronoid process was used to represent the coronoid unit, and it was chosen at the tip of the coronoid process (COR). The gonion (Go) point and anterior attachment of the masseter muscle were used to evaluate the angular growth unit of the mandible. The pogonion (Pog) point and mental foramen were selected to measure the mandibular body and chin unit, respectively (Table 1).

The method of error (E) for pointing some reference points (T, F, C, CON, COR) were calculated by Dahlberg formula as follows:

$$E = \sqrt{D^2/2N}$$

where D = difference of each measurements, N = number of measurement.

Table 2 Angular and linear measurements used in the architectural analysis

Absolute lengths	
Condyle length	A line between F and CON
Coronoid length	A line between F and COR
Angle length	A line between F and Go
Body length	A line between F and MF
Symphysis length	A line between MF and Pog
Relative lengths	
CON/COR	Condyle length/coronoid length
ANG/COR	Angle length/coronoid length
BODY/COR	Body length/coronoid length
SYM/COR	Symphysis length/coronoid length
Angles	
Condylar head axis angle	The angle between the midsagittal plane (FC-S-Ba) and the line connecting CON_l and CON_m
Condylar axis angle	The angle between the FH plane (both Or-Po) and a line connecting F-CON
Condyle–coronoid plane angle	The angle between the midsagittal plane (FC-S-Ba) and the condyle–coronoid plane (CON-COR-F)
Angular flaring angle	The angle between the midsagittal plane and the angular plane (Go-MAS_ant-F)
Ramal flaring angle	The angle between the condyle–coronoid plane (CON-COR-F) and the angular plane (Go-MAS_ant-F)

Evaluation of mandibular functional units and statistical analysis

Both sides (right and left) of each individual mandible were separately analyzed to make each data, after asymmetrical mandibles were excluded and the paired t test was made to evaluate the influence of the different side of the mandible.

The lengths, angles, and planes were measured on Coreplan 3D software using the reference points defined in the previous section. We also calculated the relative lengths of each mandibular unit relative to the length of the coronoid because the coronoid has the most consistent pattern of length and reportedly the most stable growth tendency [10].

We performed an analysis of variance (ANOVA) and Duncan's new multiple range test to compare the absolute and relative measurement between groups. All statistical analyses were performed by SAS 6.12 (SAS Institute Inc., Cary, NC, USA).

Results

When we evaluated the influence of the different side of the mandible by the paired t test, there was no significant difference in the length or angle of the right and left sides, except in the length and ratio of length of the angle in group III ($p < 0.05$; other data are not shown). So we used both sides of the mandible that the numbers of samples were doubled by pooling.

The average discrepancies in measuring the distance from the tip of the lingula or the fossa of the foramen to the condyle or coronoid tip (i.e., CON-T, COR-T, CON-F, and COR-F) ranged from 1.00 to 1.33 mm (SD=0.71 to 1.37). But the length discrepancies from the imaginary central point of the foramen entrance to the condyle or coronoid tip were somewhat larger, ranging from 1.91 to 2.48 mm (SD=1.01 to 1.77). Based on these results, point C was less reproducible than points T and F. In addition, the method of error in identifying the reference points T, F, C, CON, and COR in 3D images ranged from 0.22 to 2.98 mm with the average value of 1.22 mm.

In the linear analysis, the condyle and body length were significantly different among the three groups ($p < .0001$; Table 3). The mean condyle length was significantly longer in group III (50.5 ± 4.3 mm) than in the other groups (46.9 ± 3.9 mm for group I; 39.8 ± 3.8 mm for group II). But the coronoid length and angle length did not differ among the groups (42.3 – 43.5 and 20.2 – 22.9 mm, respectively). The symphysis length in the different groups was significantly different according to ANOVA, but not significantly different between groups I and III according to Duncan's new multiple range test.

The lengths of the mandibular units relative to the coronoid length were also significantly different for the

Table 3 The architectural analysis of the mandibular functional units by DFD groups

	Group I (n=12)	Group II (n=14)	Group III (n=34)	<i>p</i> ^a	Duncan ^b
Linear analysis of mandibular functional unit (mm)					
Condyle length	46.9±3.9	39.8±3.8	50.5±4.3	<0.0001	I ≠ II ≠ III
Coronoid length	42.3±4.6	43.3±2.1	43.5±3.4	0.5597	
Angle length	22.9±5.4	20.2±2.3	20.6±3.1	0.0994	
Body length	57.1±4.7	52.9±3.0	60.8±4.0	<0.0001	I ≠ II ≠ III
Symphysis length	29.3±2.9	27.5±1.3	31.3±3.7	0.001	I ≠ III ≠ II
Relative lengths of the units as compared with coronoid length (mm)					
Relative condyle length	1.08	0.92	1.16	<0.0001	I ≠ II ≠ III
Coronoid length	1	1	1		
Relative angle length	0.54	0.46	0.47	0.0292	II = III ≠ I
Relative body length	1.35	1.23	1.39	0.0001	I ≠ III ≠ II
Relative symphysis length	0.72	0.63	0.72	0.0019	I ≠ III ≠ II
Angular characteristics of mandibular functional unit (degree)					
Condylar head axis angle	25.3±6.2	31.0±6.2	14.9±3.7	<0.0001	I ≠ II ≠ III
Condylar axis angle	71.90±5.6	72.44±3.1	73.21±6.6	0.785	
Condyle–coronoid plane angle	14.4±3.6	17.8±3.3	11.7±2.4	<0.0001	I ≠ II ≠ III
Angular flaring angle	17.5±6.5	19.3±7.1	16.0±6.3	0.2657	
Ramal flaring angle	23.0±8.3	28.3±3.9	22.91±6.2	0.0215	I = III ≠ II

^a Analysis of variance

^b Duncan's new multiple range test

three groups, according to the ANOVA ($p < 0.05$), while Duncan's analysis verified that relative length of the condyle was the only unit that differed significantly among the groups (Table 3). The condylar head axis angle and the condyle–coronoid plane angle differed significantly among groups ($p < 0.0001$; Table 3). In addition, the condylar axis angle and the flaring angle were not significantly different among the groups ($p = 0.7850$; Table 3).

Discussion

To analyze the 3D structure of the jaw, many digital imaging modalities have been introduced, such as 3D CT, stereophotography, laser scans, and cone-beam CT [12, 13]. Developments in computer technology have also facilitated 3D simulation surgery [17], digital wafer fabrication [18], digital model surgery in virtual space [19], and navigation surgery [20]. Traditional 2D lateral cephalometry has devoted for long time to our understanding of the structural or growth-related characteristics of the craniofacial structures. For example, Singh et al. [11, 21, 22] analyzed the prognathic mandible by 2D cephalometric radiographs and spline analysis or finite element morphometry. They used some cephalometric landmarks to make the outline of the mandible, and they certainly have strong points including the big samples with the reduced radiation dose. But these

approaches are not sufficient to describe the U-shaped mandible or to analyze it with the biologically meaningful structures such as the mandibular foramen that 3D morphometry can handle with accuracy.

During 3D analysis of DFDs, the reference points should be carefully defined to represent the architecture of the craniofacial structures. The traditional reference points from 2D analysis have been generally accepted for 3D analysis without much attention to their 3D reproducibility or significance [15, 16, 23]. The transition of 2D environments to 3D for DFD will demand the turnover of our idea, reference points, planes, and analysis system by the expansion of dimension and visual field as well as the decrease of superimposition-derived landmarks.

Here, we evaluated different mandibular reference points on the 3D images; these points are generally accepted as meaningful in assessing mandibular development and functional units (Table 2). The milestone structures associated with mandibular growth are the mandibular and mental foramen, which are the first points of the mandibular ossification and located at the junction of each functional unit [5, 7].

The mandibular foramen is an entering point for the inferior alveolar bundle to the mandible and accepted as a main reference point that can express the mandibular growth units according to the functional matrix theory of Moss [1, 8, 9]. In conventional 2D analysis with panoramic

radiographs, the intersection between the central line of the mandibular canal and the perpendicular line passing through the tip of the lingula has been advocated for mandibular unit analysis [10]. However, this way of localization is not easy to apply that we initially tested three potential points in our 3D analysis to represent the exact location of the mandibular foramen: T, F, and C. In the 3D CT, points T and F were more reliable than C in terms of stability for the condyle or coronoid length because they are on the surface of the bone. But point T, on top of the lingula, did not seem to be a good reference point because of the variations in the lingula shape, which may be triangular, truncated, or nodular depending on the attachment of the sphenomandibular ligament [24]. Thus, we think that point F is a good reference point for the mandibular foramen in 3D functional unit analysis.

The mental foramen is the point where the intrauterine membranous bone formation of the mandible starts and moves toward the mandibular foramen along Meckel's cartilage. So it is closely associated with the growth of the mandibular body and is considered to be a good reference point for defining the body units. We proposed defining the mandibular body as the region between the mental and mandibular foramina, as discussed [1, 8, 9]. Therefore, we used the distance from the mental to the mandibular foramen for the mandibular body length. Kondo et al. introduced an algorithm for calculating the length of inferior alveolar nerve that it can be a useful way to analyze the mandibular body unit [25].

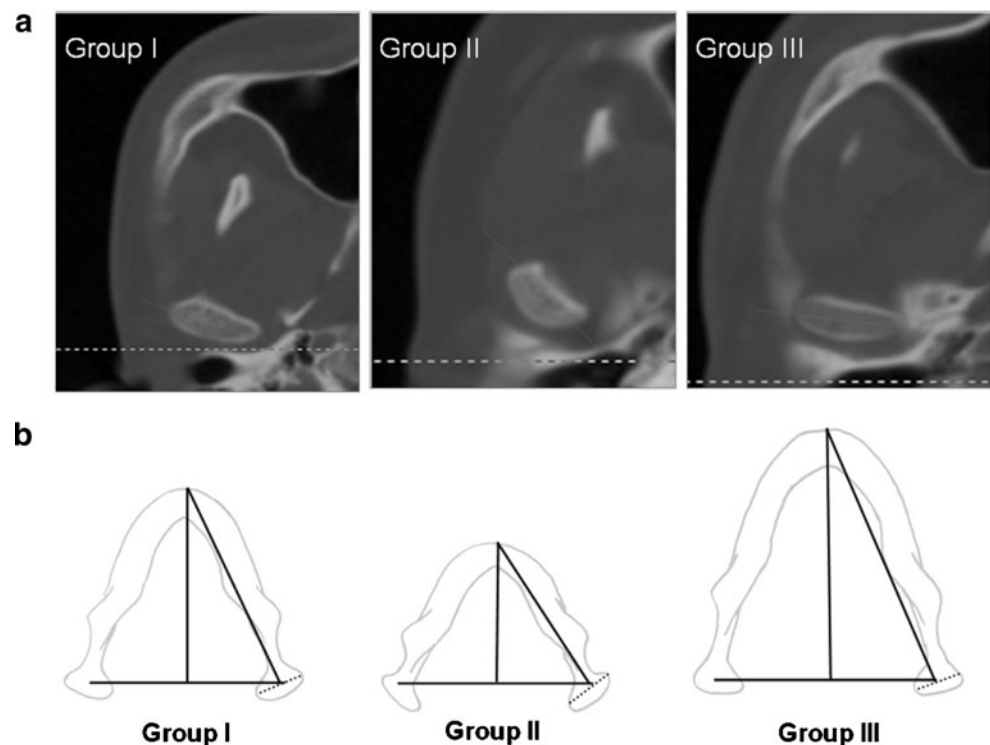
The condyle plays an important role in the mandibular growth and function [5]. The condyle has many variations in size and shape in both normal jaws and DFDs. The most superior and posterior point of the condyle has generally been used in its 2D evaluation. We used not only this point but also the medial and lateral points of the condyle to analyze its 3D structure [23, 26].

The Go is a reference points used to evaluate the mandibular angle in 2D and 3D cephalometric analysis. Both the masseter and internal pterygoid muscle attach to the mandibular angle and act as the main functional matrix for the mandibular unit of angle [26, 27]. In recent 3D studies, the anterior attachment point of the masseter muscle was introduced as a reference point for the mandibular angle [14, 16, 28], and we also used this as a reference point for the angle unit, though it is still ambiguous by its presence on the 3D curved structure.

Mandible is a bilateral structure and the right and left side were separately analyzed in this study. In order to understand the influences of the other side to the results, we performed paired sample test that the only angular unit in group III showed the side-dependent difference. We think this result does not necessarily mean not to involve the both sides of the all samples and may suggest the intrapersonal variation of angular unit in mandibular prognathism.

We analyzed and compared the characteristic pattern of functional units of normal and DFD mandibles using reference points, lengths, and angles in 3D CT. The

Fig. 2 Typical CT images and drawings of the mandible to demonstrate the architectural characteristics in normal and DFD groups. **a** Different pattern of angulations of condylar heads, revealed by the condylar head axis angle in the DFD groups. **b** A schematic presentation of the mandibular architecture with the typical condyle/body length and the condylar head axis angle



differences in the mandibular architecture between the groups with DFDs were evident in the length of the body and condyle. These lengths were the longest among patients with prognathic mandibles (group III; $p < 0.0001$) and the shortest among patients with retrognathic mandibles (group II; $p < 0.0001$; Table 3). Thus, we could think of mandibular prognathism or retrognathism as depending mainly on the length of condyle and body. Among the other mandibular units examined, the coronoid process varied the least. The condyle–coronoid plane angle was significantly different among the groups, while the angular flaring angle was not (Table 3). According to a series of studies by Singh et al. [11, 21, 22], the structural characteristics of the prognathic mandible lie in the body unit of the mandible, and these 2D cephalometric studies seem to match well with our 3D CT analysis for the prognathism. But our results indicate that the condylar unit seems to provide more etiological contribution for the prognathic morphology because the condylar unit showed the more profound and consistent elongation than the body unit when compared with normal and retrognathic group, and this difference of observations may come from the difference of the 2D vs. 3D measurement of the curved structure like mandible.

The architectural characteristics of the functional units were also examined by calculating the proportional length of each unit relative to the coronoid length [3, 10] (Table 3). The relative condyle/coronoid length was the largest in group III and the shortest in group II. This pattern was not same for the relative body/coronoid length, though this parameter was significantly longer in groups I and III than in group II.

From these results, we could deduce that the elongation or reduction of the body and condylar unit may be a good treatment strategy for mandibular retrognathism or prognathism, and it may justify the adoption of the sagittal split ramus osteotomy (SSRO) for its surgical treatment because SSRO mainly targets the body area. But this most frequently used surgical technique for mandibular retrognathism and prognathism does not change the condylar portion, and it can be an interesting point that the intraoral vertical ramus osteotomy (IVRO) that we are currently using for the prognathic mandible touches the condylar and body unit. Further studies about the structural and functional comparison of the architecture of SSRO- or IVRO-treated mandible will be necessary.

We defined the condylar axis angle as the angle between the FH plane and long axis of condyle that may represent the direction of the displacing growth of the condyle. This angle, contrary to our expectation, showed little difference among the normal and DFD mandibles. Park et al. reported that ramal inclination is different among the DFD types by 3D analysis [23]. But they used the posterior border of the mandible for the angulation of the ramus, which might be

affected by the angle region and associated muscles. We think our condylar axis angle may be a reliable indicator of the direction of condylar growth units.

The condylar head axis angle was defined as the angle between the midsagittal plane and the line connecting the medial and lateral poles of the condyle. The angle was more acute in group III (mean of 14.9°) than in group II (mean of 31.0° ; $p < 0.0001$; Fig. 2a). This difference may reflect either a condylar adaptation to the directional force of abnormal growth in DFD or an inherent condylar growth pattern to make DFD.

The architectural patterns of mandible with characteristic angles and lengths in each DFD group may be viewed as a triangle with distinct linear and angular parameters (Fig. 2b). The base of this triangle is a line connecting the centers of the left and right condyle, and the vertex is the Pog point. The condyle and body length would make up the oblique line, and the angle between the base and oblique line matches with the condylar head axis angle. Thus, the mandible in group II can be viewed as a triangle with a short oblique line and acute angle between the base and oblique line. This suggests that the mandibular architecture in group II can be expressed as a triangle with a relatively small anterior–posterior dimension by the shorter length of condyle and body unit and the more acute angle between the base and the oblique line than that of normal one (Fig. 2b), and the architecture of group III can be interpreted as a triangle with the longer oblique line by condylar unit with less acute angle.

Based on these results, we were able to define mandibular reference points for the development of functional units and characterize the 3D architecture of different types of DFD. This understanding of the differences in mandibular architecture and functional units may be helpful for the treatments of DFDs.

Acknowledgments We thank Chae-eun Lee for the technical support for the 3D imaging and Seoul C&J Inc. (Seoul, Korea) for the support of software. We also thank Dr. MK Kim and SH Kang for their profound 3D academic consultation. This work was supported by Korea Healthcare technology R&D Project, Ministry for Health, Welfare and Family Affairs (A080006), and the Korean Government (MOEHRD) KRF-2005-005-J05093 for Sang-hwy Lee.

Conflict of interest We declare that we have no conflict of interest.

References

1. Precious D, Delaire J (1987) Balanced facial growth: a schematic interpretation. *Oral Surg Oral Med Oral Pathol* 63(6):637–644
2. Hong SX, Yi CK (2001) A classification and characterization of skeletal class III malocclusion on etio-pathogenic basis. *Int J Oral Maxillofac Surg* 30(4):264–271
3. Delaire J, Schendel SA, Tulasne JF (1981) An architectural and structural craniofacial analysis: a new lateral cephalometric analysis. *Oral Surg Oral Med Oral Pathol* 52(3):226–238

4. Frost HM (2004) A 2003 update of bone physiology and Wolff's Law for clinicians. *Angle Orthod* 74(1):3–15
5. Ranly DM (1988) A synopsis of craniofacial growth, 2nd edn. Appleton & Lange, Norwalk
6. Enlow DH (1990) Facial growth, 3rd edn. Saunders, Philadelphia
7. Lee SK, Kim YS, Oh HS, Yang KH, Kim EC, Chi JG (2001) Prenatal development of the human mandible. *Anat Rec* 263(3):314–325
8. Moss ML (1968) A theoretical analysis of the functional matrix. *Acta Biotheor* 18(1):195–202
9. Moss ML, Rankow RM (1968) The role of the functional matrix in mandibular growth. *Angle Orthod* 38(2):95–103
10. Mercier J, Gordeeff A, Delaire J (1989) Le Syndrome d'insuffisance verticale postérieure unilatérale de la face, aspects cliniques et thérapeutiques. *Acta Odontol Scand* 86:13–32
11. Singh GD, McNamara JA Jr, Lozanoff S (1998) Procrustes, Euclidean and cephalometric analyses of the morphology of the mandible in human class III malocclusions. *Arch Oral Biol* 43(7):535–543
12. Hajeer MY, Millett DT, Ayoub AF, Siebert JP (2004) Applications of 3D imaging in orthodontics: part II. *J Orthod* 31(2):154–162
13. Hajeer MY, Millett DT, Ayoub AF, Siebert JP (2004) Applications of 3D imaging in orthodontics: part I. *J Orthod* 31(1):62–70
14. Katsumata A, Fujishita M, Arijji Y, Arijji E, Langlais RP (2004) 3D CT evaluation of masseter muscle morphology after setback osteotomy for mandibular prognathism. *Oral Surg Oral Med Oral Pathol Oral Radiol Endod* 98(4):461–470
15. Katsumata A, Fujishita M, Maeda M, Arijji Y, Arijji E, Langlais RP (2005) 3D-CT evaluation of facial asymmetry. *Oral Surg Oral Med Oral Pathol Oral Radiol Endod* 99(2):212–220
16. Maeda M, Katsumata A, Arijji Y, Muramatsu A, Yoshida K, Goto S, Kurita K, Arijji E (2006) 3D-CT evaluation of facial asymmetry in patients with maxillofacial deformities. *Oral Surg Oral Med Oral Pathol Oral Radiol Endod* 102(3):382–390
17. Girod S, Keeve E, Girod B (1995) Advances in interactive craniofacial surgery planning by 3D simulation and visualization. *Int J Oral Maxillofac Surg* 24(1 Pt 2):120–125
18. Kim BC, Park W, Kang YH, Yi CK, Yoo HS, Lee SH (2007) Accuracy of digital model surgery for orthognathic surgery: a preclinical evaluation. *J Korean Assoc Maxillofac Plast Reconstr Surg* 29(6):518–524
19. Swennen GR, Mollemans W, Schutyser F (2009) Three-dimensional treatment planning of orthognathic surgery in the era of virtual imaging. *J Oral Maxillofac Surg* 67(10):2080–2092
20. Tsuji M, Noguchi N, Shigematsu M, Yamashita Y, Ihara K, Shikimori M, Goto M (2006) A new navigation system based on cephalograms and dental casts for oral and maxillofacial surgery. *Int J Oral Maxillofac Surg* 35(9):828–836
21. Singh GD, McNamara JA Jr, Lozanoff S (1997) Spline analysis of the mandible in human subjects with class III malocclusion. *Arch Oral Biol* 42(5):345–353
22. Singh GD, McNamara JA Jr, Lozanoff S (1998) Mandibular morphology in subjects with class III malocclusions: finite-element morphometry. *Angle Orthod* 68(5):409–418
23. Park SH, Yu HS, Kim KD, Lee KJ, Baik HS (2006) A proposal for a new analysis of craniofacial morphology by 3-dimensional computed tomography. *Am J Orthod Dentofacial Orthop* 129(5):600.e623–600.e634
24. Tuli A, Choudhry R, Choudhry S, Raheja S, Agarwal S (2000) Variation in shape of the lingula in the adult human mandible. *J Anat* 197(Pt 2):313–317
25. Kondo T, Ong SH, Foong KW (2004) Computer-based extraction of the inferior alveolar nerve canal in 3-D space. *Comput Methods Programs Biomed* 76(3):181–191
26. Arijji Y, Kawamata A, Yoshida K, Sakuma S, Nawa H, Fujishita M, Arijji E (2000) Three-dimensional morphology of the masseter muscle in patients with mandibular prognathism. *Dentomaxillofac Radiol* 29(2):113–118
27. Pepicelli A, Woods M, Briggs C (2005) The mandibular muscles and their importance in orthodontics: a contemporary review. *Am J Orthod Dentofacial Orthop* 128(6):774–780
28. Cevidanes LH, Franco AA, Gerig G, Proffit WR, Slice DE, Enlow DH, Lederman HM, Amorim L, Scanavini MA, Vigorito JW (2005) Comparison of relative mandibular growth vectors with high-resolution 3-dimensional imaging. *Am J Orthod Dentofacial Orthop* 128(1):27–34

Copyright of Clinical Oral Investigations is the property of Springer Science & Business Media B.V. and its content may not be copied or emailed to multiple sites or posted to a listserv without the copyright holder's express written permission. However, users may print, download, or email articles for individual use.